

Large Neutrino Magnetic Dipole Moments in MSSM Extensions

Amin Aboubrahim^{b1}, Tarek Ibrahim^{a,b2}, Ahmad Itani^{b3}, and Pran Nath^{c4}

a. Department of Physics, Faculty of Science, University of Alexandria, Alexandria 21511, Egypt⁵

b. Department of Physics, Faculty of Sciences, Beirut Arab University, Beirut 11 - 5020, Lebanon⁶

c. Department of Physics, Northeastern University, Boston, MA 02115-5000, USA

Abstract

An analysis of the Dirac neutrino magnetic moment with standard model interactions gives $\mu_\nu \sim 3 \times 10^{-19} \mu_B (m_\nu / 1\text{eV})$. The observation of a significantly larger magnetic moment will provide a clear signal of new physics beyond the standard model. The current experimental limits on the neutrino magnetic moments are orders of magnitude larger than the prediction with the standard model interactions and thus its test appears out of reach. Here we give an analysis of the Dirac neutrino magnetic moments within the framework of a minimal supersymmetric standard model extension with a vectorlike lepton generation. Specifically we compute the moments arising from the exchange of W and the charged leptons in the loop, as well as from the exchange of charginos, charged sleptons and charged mirror sleptons. It is shown that the neutrino moment in this case can be several orders of magnitude larger than the one with standard model like interactions, lying close to and below the current experimental upper limits and should be accessible in improved future experiment. A correlated prediction of the heaviest neutrino lifetimes from radiative decays to the lighter neutrinos via exchange of charginos and sleptons in the loops is also made. The predicted lifetimes are several orders of magnitude smaller than the one with the standard model interactions and also lie close to the current experimental limits from analyses using the cosmic background neutrino data.

Keywords: Neutrino magnetic dipole moments, neutrino lifetime, supersymmetry, vector lepton multiplets

PACS numbers: 13.40Em, 12.60.-i, 14.60.Fg

¹Email: amin.b@bau.edu.lb

²Email: t.ibrahim@bau.edu.lb

³Email: a.itanis@bau.edu.lb

⁴Emal: nath@neu.edu

⁵Permanent address.

⁶Current address.

1 Introduction

A Dirac neutrino with standard model interactions has a magnetic moment which is given by [1]

$$\mu_{\nu_i} = \frac{3m_e G_F}{4\sqrt{2}\pi^2} m_{\nu_i} \simeq 3 \times 10^{-19} \left(\frac{m_{\nu_i}}{eV} \right) \mu_B, \quad (1)$$

where $\mu_B = e/2m_e$ is the Bohr Magneton (for related works see [2]). The observation of a neutrino magnetic moment larger than that of Eq. (1) would be a clear sign of the presence of new physics beyond the standard model. Thus a determination of the neutrino magnetic moment is of great significance in the search for physics beyond the standard model. There are a variety of experimental searches which we discuss below. Thus the Borexino experiment[3] gives an upper bound of

$$\mu_\nu \leq 5.4 \times 10^{-11} \mu_B \quad 90\% \text{ CL} . \quad (2)$$

which improves the previous limit of $8.4 \times 10^{-11} \mu_B$ found in [4]. Since Borexino explores solar neutrinos, the magnetic moment measured by Borexino is a linear combination of the magnetic moments of the three neutrino flavors. Separately the limits on e , μ and τ neutrinos are

$$\mu_{\nu_e} < 5.8 \times 10^{-11} \mu_B, \quad (3)$$

$$\mu_{\nu_\mu} < 1.5 \times 10^{-10} \mu_B, \quad (4)$$

$$\mu_{\nu_\tau} < 1.9 \times 10^{-10} \mu_B. \quad (5)$$

In reactor experiments the constraint on the neutrino magnetic moment depends on the flavor of the initial neutrino such as in $\nu_i - e$ scattering. Thus in such experiments the constraint on one flavor can be gotten⁷. The TEXONO Collaboration gives an upper limit of [5]

$$\mu_{\nu_e} < 7.4 \times 10^{-11} \mu_B, \quad 90\% \text{ CL}. \quad (6)$$

The GEMMA experiment [6] (For previous limits see [7]) gives an upper limit of

$$\mu_{\nu_e} < 2.9 \times 10^{-11} \mu_B, \quad 90\% \text{ CL} . \quad (7)$$

A more stringent limit comes from a study of the red giants at the time of helium flash, and the analysis of [8] gives a constraint on the neutrino dipole moment of

$$\mu_\nu < 3 \times 10^{-12} \mu_B, \quad (8)$$

⁷In e^+e^- annihilation process $e^+e^- \rightarrow \nu\bar{\nu}\gamma$ constraints on the neutrino magnetic moments can also be obtained but such constraints are relatively weak [9].

(which is essentially a limit on the magnetic moment μ_{ν_e}) while the Particle Data Group [9] gives a more comprehensive list of neutrino magnetic moment limits most of which, however, are not competitive with the limits in Eq. (2)-Eq. (8). Recently the authors of [10] have derived an upper bound on the Dirac neutrino magnetic moment within a low energy effective theory and obtain a limit of $\mu_\nu \leq 10^{-14} \mu_B$. The derivation assumes there be no fine-tuning of the coefficients of the operators in the effective theory. [The literature on neutrino magnetic moments is extensive. For some recent works see [11, 12, 13] and for recent reviews see [14, 15, 16]]. In any case one finds that all of the limits above whether experimental or theory are several orders of magnitude larger than the estimate of Eq. (1).

In this work we carry out an analysis of the neutrino magnetic moments in an extension of MSSM which includes a vectorlike leptonic generation which leads to significantly larger neutrino magnetic moments than given by Eq. (1). Vector like generations arise in many GUT and string models [17] and have been discussed in the literature quite frequently [18, 19, 20, 21, 22, 23, 24, 25, 26, 27, 28].

The outline of the rest of the paper is as follows: In Section 2 we describe briefly the framework of the model which is an extension of the minimal supersymmetric standard model (MSSM) including a vector leptonic multiplet. Here we define the basic interactions that mix the vector like generation with the regular three generations of leptons and sleptons. These mixings arise via the superpotential couplings as well as via soft breaking. In Section 3 we present the interactions of the neutrinos with W bosons, leptons, and their mirrors and in Section 4 we give the interactions of the neutrinos with charginos, sleptons and mirror sleptons. Using these interactions a full one loop analysis of the neutrino magnetic moments is carried out in Section 5 where the contributions from the exchange of the W and the charged leptons arise via loops shown in Fig. 1 and the contributions from the exchange of charginos, sleptons and mirror sleptons arise via loops shown in Fig. 2. In Section 6 we give a numerical analysis of the size of effects as a result of the mixing of the vectorlike generation with the three regular generations of leptons and sleptons. The analysis shows that neutrino magnetic moments as large as $(10^{-10} - 10^{-14})\mu_B$ can be gotten in models discussed in Section 5 (For large neutrino magnetic moments arising from large extra dimensions see [29, 30]). In this section we also give an evaluation of the ν_3 lifetime on which experimental lower limits exist from radiative decays of the cosmic background neutrinos. Conclusions are given in Section 7. Further details of the model are given in Section 8.

2 MSSM Extension with a vector leptonic multiplet

Vector like multiplets arise in a variety of unified models [17] some of which could be low lying. Here we simply assume the existence of one low lying leptonic vector multiplet which is anomaly free in addition to the MSSM spectrum. Before proceeding further it is useful to record the quantum numbers of the leptonic matter content of this extended MSSM spectrum under $SU(3)_C \times SU(2)_L \times U(1)_Y$. Thus under $SU(3)_C \times SU(2)_L \times U(1)_Y$ the leptons of the three generations transform as follows

$$\begin{array}{ll} \psi_{iL} \equiv \begin{pmatrix} \nu_{iL} \\ l_{iL} \end{pmatrix} & (1, 2, -\frac{1}{2}), \\ l_{iL}^c & (1, 1, 1), \\ \nu_{iL}^c & (1, 1, 0) . \end{array} \quad (9)$$

where the last entry on the right hand side column is the value of the hypercharge Y defined so that $Q = T_3 + Y$. These leptons have $V - A$ interactions. We can now add a vectorlike multiplet where we have a fourth family of leptons with $V - A$ interactions whose transformations can be gotten from Eq.(9) by letting i run from 1-4. A vectorlike lepton multiplet also has mirrors and so we consider these mirror leptons which have $V + A$ interactions. Its quantum numbers are given by

$$\begin{array}{ll} \chi^c \equiv \begin{pmatrix} E_L^c \\ N_L^c \end{pmatrix} & (1, 2, \frac{1}{2}), \\ E_L & (1, 1, -1), \\ N_L & (1, 1, 0). \end{array} \quad (10)$$

Interesting new physics arises when we allow mixings of the vectorlike generation with the three ordinary generations. Thus the superpotential of the model allowing for the mixings among the three ordinary generations and the vectorlike generation is given by

$$\begin{aligned} W = & -\mu\epsilon_{ij}\hat{H}_1^i\hat{H}_2^j + \epsilon_{ij}[f_1\hat{H}_1^i\hat{\psi}_L^j\hat{\tau}_L^c + f'_1\hat{H}_2^j\hat{\psi}_L^i\hat{\nu}_{\tau L}^c + f_2\hat{H}_1^i\hat{\chi}^{cj}\hat{N}_L + f'_2H_2^j\hat{\chi}^{ci}\hat{E}_L \\ & + h_1H_1^i\hat{\psi}_{\mu L}^j\hat{\mu}_L^c + h'_1H_2^j\hat{\psi}_{\mu L}^i\hat{\nu}_{\mu L}^c + h_2H_1^i\hat{\psi}_{eL}^j\hat{e}_L^c + h'_2H_2^j\hat{\psi}_{eL}^i\hat{\nu}_{eL}^c] \\ & + f_3\epsilon_{ij}\hat{\chi}^{ci}\hat{\psi}_L^j + f'_3\epsilon_{ij}\hat{\chi}^{ci}\hat{\psi}_{\mu L}^j + f_4\hat{\tau}_L^c\hat{E}_L + f_5\hat{\nu}_{\tau L}^c\hat{N}_L + f'_4\hat{\mu}_L^c\hat{E}_L + f'_5\hat{\nu}_{\mu L}^c\hat{N}_L \\ & + f''_3\epsilon_{ij}\hat{\chi}^{ci}\hat{\psi}_{eL}^j + f''_4\hat{e}_L^c\hat{E}_L + f''_5\hat{\nu}_{eL}^c\hat{N}_L , \end{aligned} \quad (11)$$

where $\hat{}$ implies superfields. The mass terms for the leptons and mirror leptons arise from the term

$$\mathcal{L} = -\frac{1}{2} \frac{\partial^2 W}{\partial A_i \partial A_j} \psi_i \psi_j + H.c. \quad (12)$$

where ψ and A stand for generic two-component fermion and scalar fields. After spontaneous breaking of the electroweak symmetry, ($\langle H_1^1 \rangle = v_1/\sqrt{2}$ and $\langle H_2^2 \rangle = v_2/\sqrt{2}$), we have the following set of mass terms written in the 4-component spinor notation so that

$$-\mathcal{L}_m = \bar{\xi}_R^T(M_f)\xi_L + \bar{\eta}_R^T(M_g)\eta_L + H.c., \quad (13)$$

where the basis vectors in which the mass matrix is written is given by

$$\begin{aligned} \bar{\xi}_R^T &= (\bar{\nu}_{\tau R} \quad \bar{N}_R \quad \bar{\nu}_{\mu R} \quad \bar{\nu}_{e R}), \\ \xi_L^T &= (\nu_{\tau L} \quad N_L \quad \nu_{\mu L} \quad \nu_{e L}), \\ \bar{\eta}_R^T &= (\bar{\tau}_R \quad \bar{E}_R \quad \bar{\mu}_R \quad \bar{e}_R), \\ \eta_L^T &= (\tau_L \quad E_L \quad \mu_L \quad e_L), \end{aligned} \quad (14)$$

and the mass matrix M_f is given by

$$M_f = \begin{pmatrix} f'_1 v_2/\sqrt{2} & f_5 & 0 & 0 \\ -f_3 & f_2 v_1/\sqrt{2} & -f'_3 & -f''_3 \\ 0 & f'_5 & h'_1 v_2/\sqrt{2} & 0 \\ 0 & f''_5 & 0 & h'_2 v_2/\sqrt{2} \end{pmatrix}. \quad (15)$$

The mass matrix is not hermitian and thus one needs bi-unitary transformations to diagonalize it. We define the bi-unitary transformation so that

$$D_R^{\nu\dagger}(M_f)D_L^\nu = \text{diag}(m_{\psi_1}, m_{\psi_2}, m_{\psi_3}, m_{\psi_4}). \quad (16)$$

Under the bi-unitary transformations the basis vectors transform so that

$$\begin{pmatrix} \nu_{\tau R} \\ N_R \\ \nu_{\mu R} \\ \nu_{e R} \end{pmatrix} = D_R^\nu \begin{pmatrix} \psi_{1R} \\ \psi_{2R} \\ \psi_{3R} \\ \psi_{4R} \end{pmatrix}, \quad \begin{pmatrix} \nu_{\tau L} \\ N_L \\ \nu_{\mu L} \\ \nu_{e L} \end{pmatrix} = D_L^\nu \begin{pmatrix} \psi_{1L} \\ \psi_{2L} \\ \psi_{3L} \\ \psi_{4L} \end{pmatrix}. \quad (17)$$

In Eq. (16) $\psi_1, \psi_2, \psi_3, \psi_4$ are the mass eigenstates for the neutrinos, where in the limit of no mixing we identify ψ_1 as the light tau neutrino, ψ_2 as the heavier mass eigen state, ψ_3 as the muon neutrino

and ψ_4 as the electron neutrino. To make contact with the normal neutrino hierarchy we relabel the states so that

$$\nu_1 = \psi_4, \nu_2 = \psi_3, \nu_3 = \psi_1, \nu_4 = \psi_2, \quad (18)$$

which we assume has the mass hierarchical pattern

$$m_{\nu_1} < m_{\nu_2} < m_{\nu_3} < m_{\nu_4}. \quad (19)$$

We will carry out the analytical analysis in the ψ_i notation but the numerical analysis will be carried out in the ν_i notation to make direct contact with data. A similar analysis goes to the lepton mass matrix M_ℓ where

$$M_\ell = \begin{pmatrix} f_1 v_1 / \sqrt{2} & f_4 & 0 & 0 \\ f_3 & f'_2 v_2 / \sqrt{2} & f'_3 & f''_3 \\ 0 & f'_4 & h_1 v_1 / \sqrt{2} & 0 \\ 0 & f''_4 & 0 & h_2 v_1 / \sqrt{2} \end{pmatrix}. \quad (20)$$

Next we consider the mixing of the charged sleptons and the charged mirror sleptons. The mass squared matrix of the slepton - mirror slepton comes from three sources: the F term, the D term of the potential and the soft susy breaking terms. Using the superpotential of Eq. (11) the mass terms arising from it after the breaking of the electroweak symmetry are given by the Lagrangian

$$\mathcal{L} = \mathcal{L}_F + \mathcal{L}_D + \mathcal{L}_{\text{soft}}, \quad (21)$$

where \mathcal{L}_F is deduced from Eq. (11) and is given in the Appendix, while the \mathcal{L}_D is given by

$$\begin{aligned} -\mathcal{L}_D = & \frac{1}{2} m_Z^2 \cos^2 \theta_W \cos 2\beta \{ \tilde{\nu}_{\tau L} \tilde{\nu}_{\tau L}^* - \tilde{\tau}_L \tilde{\tau}_L^* + \tilde{\nu}_{\mu L} \tilde{\nu}_{\mu L}^* - \tilde{\mu}_L \tilde{\mu}_L^* + \tilde{\nu}_{e L} \tilde{\nu}_{e L}^* - \tilde{e}_L \tilde{e}_L^* \\ & + \tilde{E}_R \tilde{E}_R^* - \tilde{N}_R \tilde{N}_R^* \} + \frac{1}{2} m_Z^2 \sin^2 \theta_W \cos 2\beta \{ \tilde{\nu}_{\tau L} \tilde{\nu}_{\tau L}^* + \tilde{\tau}_L \tilde{\tau}_L^* + \tilde{\nu}_{\mu L} \tilde{\nu}_{\mu L}^* + \tilde{\mu}_L \tilde{\mu}_L^* \\ & + \tilde{\nu}_{e L} \tilde{\nu}_{e L}^* + \tilde{e}_L \tilde{e}_L^* - \tilde{E}_R \tilde{E}_R^* - \tilde{N}_R \tilde{N}_R^* + 2\tilde{E}_L \tilde{E}_L^* - 2\tilde{\tau}_R \tilde{\tau}_R^* - 2\tilde{\mu}_R \tilde{\mu}_R^* - 2\tilde{e}_R \tilde{e}_R^* \}. \end{aligned} \quad (22)$$

For $\mathcal{L}_{\text{soft}}$ we assume the following form

$$\begin{aligned} -\mathcal{L}_{\text{soft}} = & \tilde{M}_{\tau L}^2 \tilde{\psi}_{\tau L}^{i*} \tilde{\psi}_{\tau L}^i + \tilde{M}_{\chi}^2 \tilde{\chi}^{ci*} \tilde{\chi}^{ci} + \tilde{M}_{\mu L}^2 \tilde{\psi}_{\mu L}^{i*} \tilde{\psi}_{\mu L}^i + \tilde{M}_{e L}^2 \tilde{\psi}_{e L}^{i*} \tilde{\psi}_{e L}^i + \tilde{M}_{\nu_\tau}^2 \tilde{\nu}_{\tau L}^{c*} \tilde{\nu}_{\tau L}^c + \tilde{M}_{\nu_\mu}^2 \tilde{\nu}_{\mu L}^{c*} \tilde{\nu}_{\mu L}^c \\ & + \tilde{M}_{\nu_e}^2 \tilde{\nu}_{e L}^{c*} \tilde{\nu}_{e L}^c + \tilde{M}_\tau^2 \tilde{\tau}_L^{c*} \tilde{\tau}_L^c + \tilde{M}_\mu^2 \tilde{\mu}_L^{c*} \tilde{\mu}_L^c + \tilde{M}_e^2 \tilde{e}_L^{c*} \tilde{e}_L^c + \tilde{M}_E^2 \tilde{E}_L^* \tilde{E}_L + \tilde{M}_N^2 \tilde{N}_L^* \tilde{N}_L \\ & + \epsilon_{ij} \{ f_1 A_\tau H_1^i \tilde{\psi}_{\tau L}^j \tilde{\tau}_L^c - f'_1 A_{\nu_\tau} H_2^i \tilde{\psi}_{\tau L}^j \tilde{\nu}_{\tau L}^c + h_1 A_\mu H_1^i \tilde{\psi}_{\mu L}^j \tilde{\mu}_L^c - h'_1 A_{\nu_\mu} H_2^i \tilde{\psi}_{\mu L}^j \tilde{\nu}_{\mu L}^c \\ & + h_2 A_e H_1^i \tilde{\psi}_{e L}^j \tilde{e}_L^c - h'_2 A_{\nu_e} H_2^i \tilde{\psi}_{e L}^j \tilde{\nu}_{e L}^c + f_2 A_N H_1^i \tilde{\chi}^{cj} \tilde{N}_L - f'_2 A_E H_2^i \tilde{\chi}^{cj} \tilde{E}_L + H.c. \}. \end{aligned} \quad (23)$$

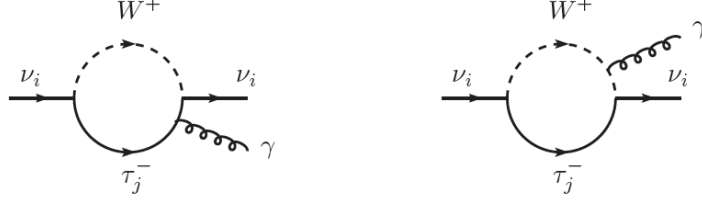


Figure 1: The diagrams that contribute to neutrino magnetic dipole moment via exchange of the W boson and of the leptons and of the mirror leptons where the photon is either emitted by the W boson (right) or by the lepton or by the mirror lepton (left) inside the loop.

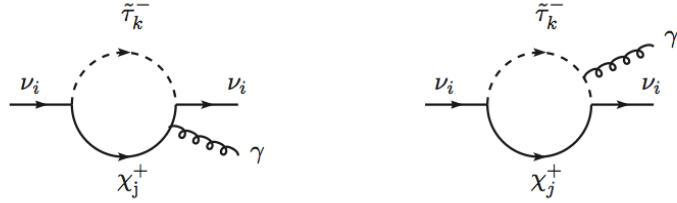


Figure 2: The diagrams that contribute to neutrino magnetic dipole moment via supersymmetric loops involving the exchange of charginos and of sleptons and mirror sleptons where the photon is either emitted by the chargino (left) or by the slepton or by the mirror slepton (right) inside the loop.

3 Interactions of W boson, leptons, mirrors and neutrinos

The magnetic dipole moments of the neutrinos arise from the loop diagrams of Fig. 1 and Fig. 2. We now write the charged current interaction in the leptonic sector for the three generations and for the mirror generation with the W boson,

$$-\mathcal{L}_{CC} = \frac{g}{2\sqrt{2}} W_\rho^\dagger \{ \bar{\nu}_\tau \gamma^\rho (1 - \gamma_5) \tau + \bar{\nu}_\rho \gamma^\rho (1 - \gamma_5) \mu + \bar{\nu}_e \gamma^\rho (1 - \gamma_5) e + \bar{N} \gamma^\rho (1 + \gamma_5) E \} + H.c. \quad (24)$$

Using Eq.17, and its counterpart in the lepton sector, one can write the charged current interactions in the mass diagonal basis as

$$-\mathcal{L}_{CC} = \frac{g}{2\sqrt{2}} W_\rho^\dagger \sum_{i=1}^4 \sum_{j=1}^4 \bar{\psi}_i \gamma^\rho \{ (D_{L1i}^{\nu*} D_{L1j}^\tau + D_{L3i}^{\nu*} D_{L3j}^\tau + D_{L4i}^{\nu*} D_{L4j}^\tau)(1 - \gamma_5) + (D_{R2i}^{\nu*} D_{R2j}^\tau)(1 + \gamma_5) \} \tau_j + H.c.. \quad (25)$$

4 Interactions of charginos, sleptons and neutrinos

The magnetic dipole moments of the neutrinos arise from loop diagrams of Fig.2. The relevant part of the Lagrangian that generates this contribution is given by

$$-\mathcal{L}_{\nu-\tilde{\tau}-\chi^+} = \sum_{i=1}^4 \sum_{j=1}^2 \sum_{k=1}^8 \bar{\psi}_i [C_{ijk}^L P_L + C_{ijk}^R P_R] \tilde{\chi}_j^+ \tilde{\tau}_k + H.c. \quad (26)$$

where

$$\begin{aligned} C_{ijk}^L &= -f'_1 V_{j2}^* D_{R_{1i}}^{\nu*} \tilde{D}_{1k}^\tau - f'_2 V_{j2}^* D_{R_{2i}}^{\nu*} \tilde{D}_{2k}^\tau + g V_{j1}^* D_{R_{2i}}^{\nu*} \tilde{D}_{4k}^\tau - h'_1 V_{j2}^* D_{R_{3i}}^{\nu*} \tilde{D}_{5k}^\tau - h'_2 V_{j2}^* D_{R_{4i}}^{\nu*} \tilde{D}_{7k}^\tau, \\ C_{ijk}^R &= -f_1 U_{j2} D_{L_{1i}}^{\nu*} \tilde{D}_{3k}^\tau - h_1 U_{j2} D_{L_{3i}}^{\nu*} \tilde{D}_{6k}^\tau + g U_{j1} D_{L_{1i}}^{\nu*} \tilde{D}_{1k}^\tau + g U_{j1} D_{L_{4i}}^{\nu*} \tilde{D}_{7k}^\tau \\ &\quad - h_2 U_{j2} D_{L_{4i}}^{\nu*} \tilde{D}_{8k}^\tau - f_2 U_{j2} D_{L_{2i}}^{\nu*} \tilde{D}_{4k}^\tau, \end{aligned} \quad (27)$$

where \tilde{D}^τ is the diagonalizing matrix of the scalar mass squared matrix for the scalar leptons as defined in the Appendix. In Eq.(27) U and V are the matrices that diagonalize the chargino mass matrix M_C so that

$$U^* M_C V^{-1} = \text{diag}(m_{\tilde{\chi}_1^+}^+, m_{\tilde{\chi}_2^+}^+). \quad (28)$$

5 An analytical computation of the neutrino magnetic moments

The dipole moments for neutrinos are defined by

$$\langle \nu_j(p') | J_\alpha^{em} | \nu_i(p) \rangle = \mu_\nu^m(q^2)_{ij} \bar{u}_j(p') i\sigma_{\alpha\rho} q^\rho u_i(p) + d_\nu^e(q^2)_{ij} \bar{u}_j(p') i\sigma_{\alpha\rho} \gamma_5 q^\rho u_i(p) + \dots \quad (29)$$

where $\mu_\nu^m(q^2)_{ij}$ is the magnetic dipole form factor and $d_\nu^e(q^2)_{ij}$ is the electric dipole form factor. We are interested in their values at zero momentum transfer, i.e., the quantities $\mu_\nu^m(0)_{ij}$, $d_\nu^e(0)_{ij}$. For the case when $i = j$ these moments vanish if the neutrino is a Majorana field, but is in general non-vanishing for a Dirac neutrino. When $i \neq j$ one has transition moments and they can be non-vanishing both for Dirac as well as for Majorana neutrinos. The analysis given below is general in that we consider the lepton and the neutrino mass mixings which form 4×4 matrices while the slepton mass squares form an 8×8 matrix. A sub case was previously considered in [20] where only the tau neutrino magnetic moment was computed while the analysis given here is more general.

We now give a computation of the magnetic dipole moment arising from the loop diagrams of Fig.1 and Fig. 2. First the W boson loops of Fig. 1 produce the following contribution to the

magnetic moment μ_i of the neutrino ψ_i in Bohr magneton units $\mu_B (= e/2m_e)$ so that

$$\begin{aligned} \mu_i^W = & -\frac{g^2 m_e}{64\pi^2 M_W^2} \sum_{j=1}^4 m_{\tau_j} [|v_{ij}|^2 - |a_{ij}|^2] G_1\left(\frac{m_{\tau_j}}{M_W}\right) + \\ & \frac{3g^2 m_e m_{\psi_i}}{128\pi^2 M_W^2} \sum_{j=1}^4 [|v_{ij}|^2 + |a_{ij}|^2] G_2\left(\frac{m_{\tau_j}}{M_W}\right), \end{aligned} \quad (30)$$

where

$$\begin{aligned} v_{ij} = & D_{L1i}^{\nu*} D_{L1j}^\tau + D_{L3i}^{\nu*} D_{L3j}^\tau + D_{L4i}^{\nu*} D_{L4j}^\tau + D_{R2i}^{\nu*} D_{R2j}^\tau, \\ a_{ij} = & D_{L1i}^{\nu*} D_{L1j}^\tau + D_{L3i}^{\nu*} D_{L3j}^\tau + D_{L4i}^{\nu*} D_{L4j}^\tau - D_{R2i}^{\nu*} D_{R2j}^\tau. \end{aligned} \quad (31)$$

The chargino exchange loops of Fig. 2 produce a contribution to the magnetic moments of the neutrinos in μ_B units so that

$$\mu_i^\chi = \frac{m_e}{16\pi^2} \sum_{j=1}^2 \sum_{k=1}^8 \frac{1}{m_{\chi_j}} [|v_{ijk}|^2 - |a_{ijk}|^2] G_3\left(\frac{m_{\tilde{\tau}_k}}{m_{\chi_j}}\right) + \frac{m_e m_{\psi_i}}{48\pi^2} [|v_{ijk}|^2 + |a_{ijk}|^2] G_4\left(\frac{m_{\tilde{\tau}_k}}{m_{\chi_j}}\right), \quad (32)$$

where

$$\begin{aligned} v_{ijk} = & \frac{1}{2} \{C_{ijk}^L + C_{ijk}^R\}, \\ a_{ijk} = & \frac{1}{2} \{C_{ijk}^L - C_{ijk}^R\}. \end{aligned} \quad (33)$$

The form factors $G_i(x)$ are given by

$$\begin{aligned} G_1(x) = & \frac{4-x^2}{1-x^2} + \frac{3x^2}{(1-x^2)^2} \ln(x^2), \\ G_2(x) = & \frac{2-5x^2+x^4}{(1-x^2)^2} - \frac{2x^4}{(1-x^2)^3} \ln(x^2), \\ G_3(x) = & \frac{-2}{x^2-1} + \frac{2x^2}{(x^2-1)^2} \ln(x^2), \\ G_4(x) = & \frac{3(1+x^2)}{(1-x^2)^2} + \frac{6x^2}{(1-x^2)^3} \ln(x^2). \end{aligned} \quad (34)$$

The form factors G_1 and G_2 arise from the non-supersymmetric loops of Fig. 1 involving the exchange of the W boson and the charged leptons while the form factors G_3 and G_4 arise from the supersymmetric loops of Fig. 2 from the exchange of the charginos and the charged sleptons.

6 Numerical analysis and results

In this section we give a numerical analysis for the magnetic moment of the electron (μ_1) and for the muon (μ_2). In the analysis we will impose the constraint on the sum of the neutrino masses arising from the Planck Satellite experiment [31] so that

$$\sum_{i=1}^3 m_{\nu_i} < 0.85 eV , \quad (35)$$

where we assume ν_i ($i=1,2,3$) to be the mass eigenstates with eigenvalues m_{ν_i} with the mass hierarchy given in Eq. (18). Neutrino oscillations constraint the neutrino mass squared differences so that [32]

$$\Delta m_{31}^2 \equiv m_3^2 - m_1^2 = 2.4_{-0.11}^{+0.12} \times 10^{-3} eV^2 , \quad (36)$$

$$\Delta m_{21}^2 \equiv m_2^2 - m_1^2 = 7.65_{-0.20}^{+0.23} \times 10^{-5} eV^2 . \quad (37)$$

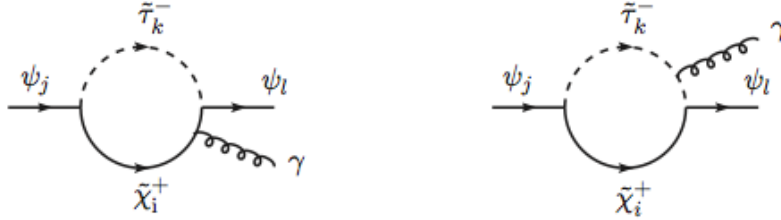


Figure 3: Neutrino radiative decay $\psi_j \rightarrow \psi_l + \gamma$ via supersymmetric loops involving the charginos and the sleptons by the emission of the photon from either the chargino (left) or by the slepton (right) inside the loop.

It is also interesting to include in the analysis of the neutrino magnetic moments the prediction of the neutrino lifetime for the decay $\nu_3 \rightarrow \nu_1 \gamma, \nu_2 \gamma$ (see Fig. 3). A computation of the neutrino lifetime with the standard model interactions gives [33]

$$\tau_{\nu_3}^{SM} \sim 10^{43} \text{ yrs}, \quad (38)$$

for a ν_3 with mass 50 meV. One may compare this with the experimental data from galaxy surveys within frared satellites AKARI [34], Spitzer [35] and Hershel [36] as well as the high precision cosmic microwave background (CMB) data collected by the Far Infrared Absolute Spectrometer (FIRAS)

on board the Cosmic Background explorer (COBE) [37] for the study of radiative decays of the cosmic neutrinos[38] using the Cosmic Infrared Background (CIB) which gives [38]

$$\tau_{\nu_3}^{exp} \geq 10^{12} \text{ yrs} . \quad (39)$$

A lifetime orders of magnitude smaller than that of Eq.(38) was shown to arise in the analysis of [18]. In the analysis of ν_3 lifetime here we will use the formulae derived in [18]. As in [18] we will see that similar size lifetimes also arise with the inputs used in the analysis of the neutrino magnetic dipole moments presented here.

In Table 1 we give the analysis of neutrino masses for four sets of inputs. For each set of inputs, in addition to the muon and the electron neutrino magnetic moments, we also display the ν_3 lifetime as well as the lighter chargino and slepton masses that enter the loops. The computed values of the tau neutrino lifetime are consistent with the analysis of [18]. From Table 1 it is clear that μ_2 can lie close to $\mathcal{O}(10^{-10})\mu_B$ which is the current experimental limit. Further μ_1 can be $\mathcal{O}(10^{-12})\mu_B$. Both μ_1 and μ_2 are several orders in magnitude greater than that predicted by the Standard Model type interactions.

Neutrino Mass Eigenvalues (GeV)		$m_{\nu_3} = 5.2 \times 10^{-11}$ $m_{\nu_2} = 9.2 \times 10^{-12}$ $m_{\nu_1} = 9.7 \times 10^{-13}$
(i) $m_{\chi^\pm} = 256$ GeV $m_{\tilde{\tau}} = 162$ GeV	μ_2	1.2×10^{-10}
	μ_1	2.5×10^{-13}
	ν_3 lifetime	3.9×10^{14} yrs
(ii) $m_{\chi^\pm} = 267$ GeV $m_{\tilde{\tau}} = 202$ GeV	μ_2	4.6×10^{-10}
	μ_1	1.3×10^{-12}
	ν_3 lifetime	2.5×10^{14} yrs
(iii) $m_{\chi^\pm} = 268$ GeV $m_{\tilde{\tau}} = 158$ GeV	μ_2	2.2×10^{-10}
	μ_1	1.1×10^{-13}
	ν_3 lifetime	1.8×10^{14} yrs
(iv) $m_{\chi^\pm} = 272$ GeV $m_{\tilde{\tau}} = 195$ GeV	μ_2	-7.6×10^{-10}
	μ_1	-1.3×10^{-13}
	ν_3 lifetime	8.8×10^{13} yrs

Table 1: An exhibition of the numerical values for the muon neutrino magnetic moment μ_2 and of the electron neutrino magnetic moment μ_1 for four sets of inputs (i)-(iv). The common parameter for the four sets are: $|f_3| = 7 \times 10^{-8}$, $|f'_3| = 5 \times 10^{-8}$, $|f''_3| = 8 \times 10^{-9}$, $|f'_4| = |f''_4| = 42$, $|f_5| = 8.11 \times 10^{-2}$, $|f'_5| = 9.8 \times 10^{-2}$, $|f''_5| = 4 \times 10^{-2}$, $m_N = 212$, $\tan \beta = 60$, $\chi_3 = 0.3$, $\chi'_3 = 0.2$, $\chi''_3 = 0.6$, $\chi_4 = 3.1$, $\chi'_4 = 0.1$, $\chi''_4 = 0.5$, $\chi_5 = 1.9$, $\chi'_5 = 0.5$ and $\chi''_5 = 0.7$. Additional parameters which are different for different sets are as follows: Set (i): $m_E = 460$, $m_0 = 300$, $A_0 = 579$, $m_2 = 320$, $\mu = 300$ and $|f_4| = 65$. Set (ii): $m_E = 550$, $m_0 = 300$, $A_0 = 600$, $m_2 = 350$, $\mu = 300$ and $|f_4| = 65$. Set (iii): $m_E = 550$, $m_0 = 305$, $A_0 = 650$, $m_2 = 355$, $\mu = 300$ and $|f_4| = 65$. Set (iv): $m_E = 703$, $m_0 = 335$, $A_0 = 780$, $m_2 = 320$, $\mu = 305$ and $|f_4| = 64$. All masses are in GeV, phases in rad and magnetic moments in units of μ_B . The neutrino mass eigenvalues and the ν_3 lifetime are also exhibited.

Fig. 4 displays the neutrino magnetic moments μ_1 and μ_2 as a function of the soft $SU(2)$ gaugino mass m_2 . The gaugino mass m_2 enters the analysis via the chargino mass matrix. The analysis of Fig. 4 is for three values of $\tan \beta$ which from top to bottom are 40, 50 and 60 which correspond to the unmarked solid, long -dashed and short-dashed curves. We note that the largest contribution to the magnetic moments arise from the supersymmetric sector, i.e., from the chargino exchange loop diagrams while the W exchange loop diagrams make a negligible contribution. Fig. 4 shows that μ_2 can be $\mathcal{O}(10^{-10}\mu_B)$ and the predicted values fall below but are close to the experimental upper limit. As for μ_1 , the predicted values can reach $\sim 10^{-13}\mu_B$ which is clearly a major enhancement on what is predicted by the Standard Model like interactions. The ν_3 lifetime corresponding to the cases $\tan \beta = 40, 50, 60$ is also exhibited by the marked curves.

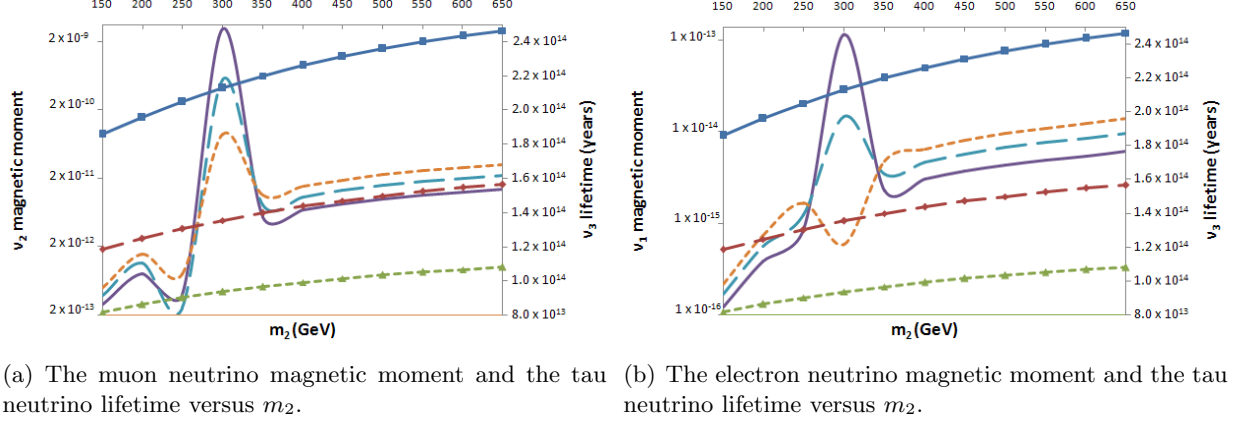
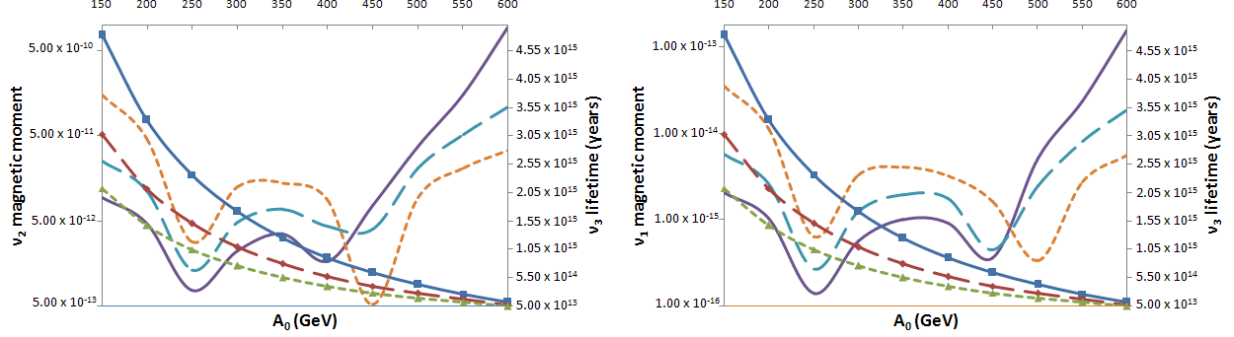


Figure 4: A display of the neutrino magnetic moments (unmarked solid, long dashed and short dashed) and the ν_3 lifetime (marked solid, long dashed and short dashed) as a function of the gaugino mass m_2 in the range 150-650 GeV. The three sets of curves correspond to $\tan \beta = 40$ (solid curve), $\tan \beta = 50$ (long dashed), and $\tan \beta = 60$ (short dashed). Other parameters have the values $\mu = 100$, $|f_3| = 7 \times 10^{-8}$, $|f'_3| = 5 \times 10^{-8}$, $|f''_3| = 8 \times 10^{-9}$, $|f_4| = 57$, $|f'_4| = 42$, $|f''_4| = 42$, $|f_5| = 8.11 \times 10^{-2}$, $|f'_5| = 9.8 \times 10^{-2}$, $|f''_5| = 4 \times 10^{-2}$, $m_N = 212$, $A_0 = 570$, $m_E = 360$, $m_0 = 300$, $\chi_3 = 0.3$, $\chi'_3 = 0.2$, $\chi''_3 = 0.6$, $\chi_4 = 2.8$, $\chi'_4 = 0.1$, $\chi''_4 = 0.5$, $\chi_5 = 1.9$, $\chi'_5 = 0.5$ and $\chi''_5 = 0.7$. All masses are in GeV and the phases in rad.

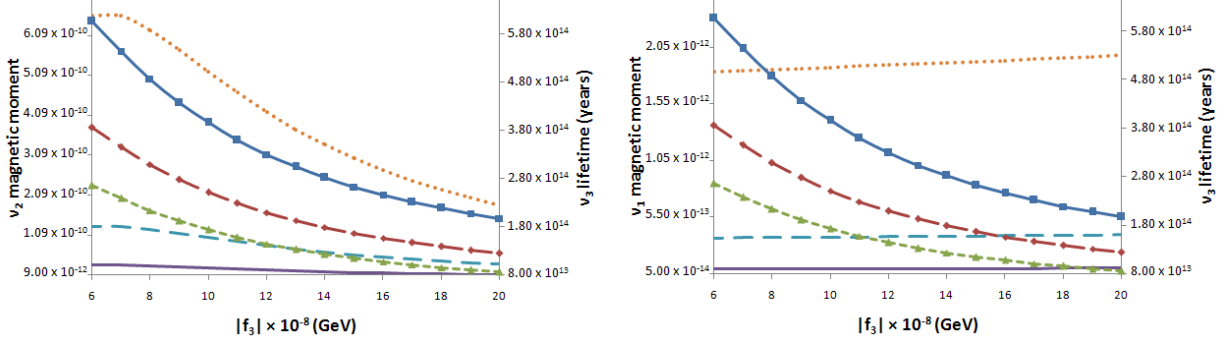
Fig. 5 exhibits the variation of the neutrinos magnetic moments with the trilinear coupling A_0 in the range 150 – 600 GeV where in the analysis we assumed $A_\tau = A_E = A_\mu = A_e = A_0$. The trilinear coupling appears in the slepton mass squared matrix and thus affects the chargino-slepton loop contribution. As in Fig. 4 the magnetic moment analysis corresponding to $\tan \beta = 40, 50, 60$ are displayed while the corresponding analysis for the ν_3 lifetime are exhibited by marked lines. A sample point in the analysis is $\tan \beta = 50$ (long-dashed curve) and $A_0 = 600$ GeV where μ_2 takes a value $\sim 1.1 \times 10^{-10} \mu_B$ and $\tau_{\nu_3} \sim 7 \times 10^{13}$ yrs.



(a) The muon neutrino magnetic moment and the tau neutrino lifetime versus A_0 . (b) The electron neutrino magnetic moment and the tau neutrino lifetime versus A_0 .

Figure 5: A display of the neutrino magnetic moments and ν_3 lifetime as a function of the trilinear coupling A_0 in the range 150-600 GeV. The left panel gives the ν_2 magnetic moment and the right panel gives the ν_1 magnetic moment along with the ν_3 lifetime. The curves correspond to $\tan \beta = 40$ (solid), $\tan \beta = 50$ (long dashed), and $\tan \beta = 60$ (short dashed). The marked curves correspond to the ν_3 lifetime. Other parameters have the values $m_2 = 297.8$, $\mu = 100$, $|f_3| = 7 \times 10^{-8}$, $|f'_3| = 5 \times 10^{-8}$, $|f''_3| = 8 \times 10^{-9}$, $|f_4| = 57$, $|f'_4| = 42$, $|f''_4| = 42$, $|f_5| = 8.11 \times 10^{-2}$, $|f'_5| = 9.8 \times 10^{-2}$, $|f''_5| = 4 \times 10^{-2}$, $m_N = 212$, $m_E = 360$, $m_0 = 300$, $\chi_3 = 0.3$, $\chi'_3 = 0.2$, $\chi''_3 = 0.6$, $\chi_4 = 3.1$, $\chi'_4 = 0.1$, $\chi''_4 = 0.5$, $\chi_5 = 1.9$, $\chi'_5 = 0.5$ and $\chi''_5 = 0.7$. All masses are in GeV and the phases in rad.

Fig. 6 exhibits the variation of the neutrino magnetic moments versus the magnitude of the coupling f_3 for $\tan \beta = 40, 50, 60$ starting from the bottom solid curve going to the top short-dashed curve. As in the previous figures the unmarked curves are for the neutrinos magnetic moments while the marked ones are for the ν_3 lifetime. The analysis of the figure shows that the muon neutrino magnetic moment can take values of the order of $10^{-10} \mu_B$ while the electron neutrino magnetic moment can reaches values $\sim 2 \times 10^{-12} \mu_B$. Also as in the previous case the constraints on Δm_{31}^2 , Δm_{21}^2 , and on the sum of the neutrino masses must be satisfied. An example of such a point is $|f_3| = 7 \times 10^{-8}$ GeV and $\tan \beta = 60$, which gives $\mu_2 = 6.6 \times 10^{-10} \mu_B$, $\mu_1 = 1.9 \times 10^{-12} \mu_B$ and $\tau_{\nu_3} = 2.4 \times 10^{14}$ yrs. It is worth noting that μ_1 is not affected much by the change in $|f_3|$ as can be seen from the graph, where the curves are almost horizontal straight lines.



(a) The muon neutrino magnetic moment and tau neutrino lifetime versus $|f_3|$. (b) The electron neutrino magnetic moment and the tau neutrino lifetime versus $|f_3|$.

Figure 6: A display of the neutrino magnetic moments and the ν_3 lifetime as a function of $|f_3|$. The left panel gives the ν_2 magnetic moment while the right panel gives the ν_1 magnetic moment along with the ν_3 lifetime. The three curves correspond to the values of $\tan \beta = 40$ (solid curve), $\tan \beta = 50$ (dashed), and $\tan \beta = 60$ (dotted). The marked curves correspond to the ν_3 lifetime. Other parameters have the values $m_2 = 250$, $\mu = 100$, $|f'_3| = 5 \times 10^{-8}$, $|f''_3| = 8 \times 10^{-9}$, $|f_4| = 55$, $|f'_4| = 42$, $|f''_4| = 42$, $|f_5| = 8.11 \times 10^{-2}$, $|f'_5| = 9.8 \times 10^{-2}$, $|f''_5| = 4 \times 10^{-2}$, $m_N = 212$, $m_E = 360$, $m_0 = 300$, $\chi_3 = 0.3$, $\chi'_3 = 0.2$, $\chi''_3 = 0.6$, $\chi_4 = 1.8$, $\chi'_4 = 2.9$, $\chi''_4 = 0.5$, $\chi_5 = 1.9$, $\chi'_5 = 0.5$, $\chi''_5 = 0.7$ and $A_0 = 579$. All masses are in GeV and the phases in rad.

Next we study the effect of CP phases on the magnetic moment and on the ν_3 lifetime (for a review see [39]). Thus, e.g., in [40] the dependence of the muon magnetic moment on CP phases was investigated and its sharp dependence on several CP phases in MSSM was found. Thus we expect that here also the neutrino magnetic moments will be sensitive to the CP phases. We begin by defining the CP phases χ_i and χ'_i ($i=1-5$) by

$$f_i = |f_i|e^{i\chi_i}, \quad f'_i = |f'_i|e^{i\chi'_i}, \quad i = 3 - 5. \quad (40)$$

In Fig. 7 we exhibit the dependence of the magnetic moments and of the ν_3 lifetime on the CP phase χ_4 . The coupling f_4 appears in the lepton mass matrix and in the slepton mass squared matrix and thus the phase enters in the W exchange contribution as well as in the chargino exchange contribution to the magnetic moment. Variation of χ_4 has no influence on the neutrino mass matrix. Fig. 7 exhibits the variation of μ_1 and μ_2 and of ν_3 lifetime with χ_4 for three values of m_E , i.e., for $m_E = 360, 460$ and 560 GeV starting from the solid curve down to the short-dashed curve. It is seen that significantly larger magnetic moments and significantly smaller ν_3 lifetime relative to the standard model case are obtained as in the previous cases.

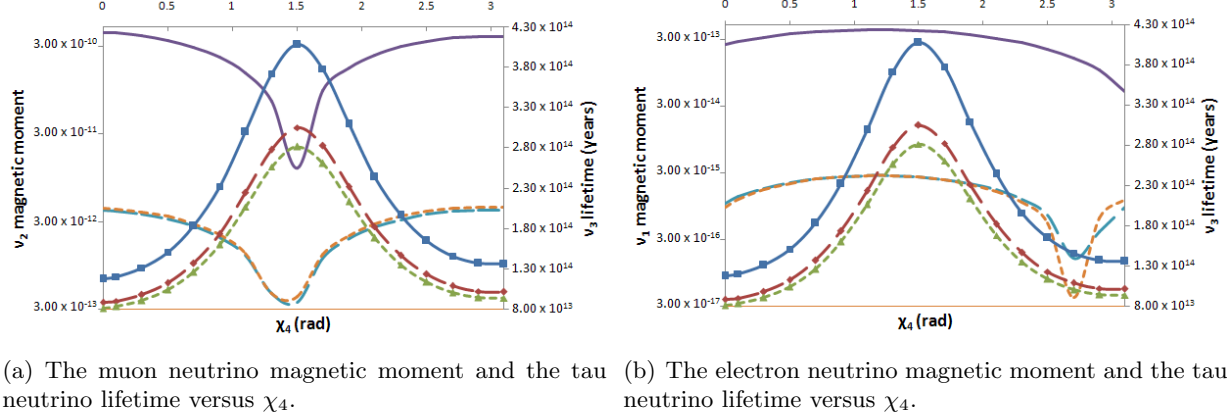
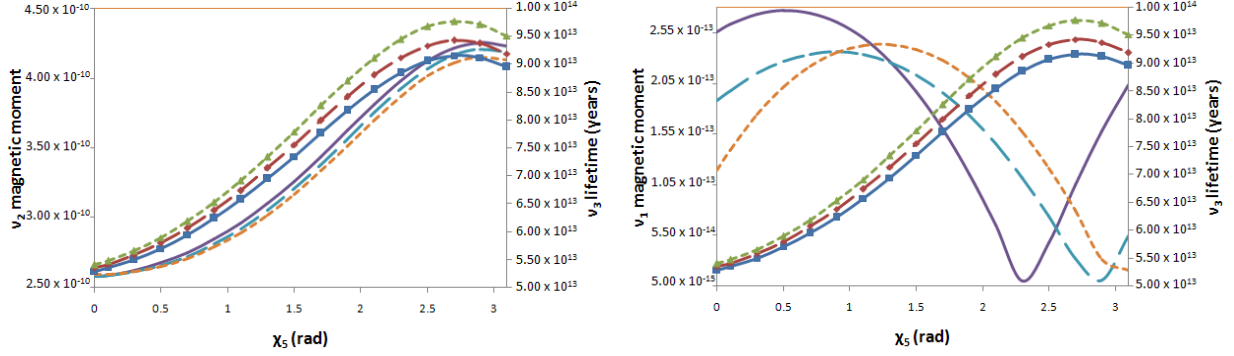


Figure 7: A display of the neutrino magnetic moments and the ν_3 lifetime as a function of the phase χ_4 . The left panel shows the ν_2 magnetic moment and the right panel shows the ν_1 magnetic moment along with the ν_3 lifetime. The three curves correspond to the values of $m_E = 360$ (solid curve), $m_E = 460$ (long dashed), and $m_E = 560$ (short dashed). The marked curves correspond to the ν_3 lifetime. Other parameters have the values $m_2 = 250$, $\mu = 100$, $|f_3| = 7 \times 10^{-8}$, $|f'_3| = 5 \times 10^{-8}$, $|f''_3| = 8 \times 10^{-9}$, $|f_4| = 55$, $|f'_4| = 42$, $|f''_4| = 42$, $|f_5| = 8.11 \times 10^{-2}$, $|f'_5| = 9.8 \times 10^{-2}$, $|f''_5| = 4 \times 10^{-2}$, $m_N = 212$, $m_0 = 300$, $A_0 = 579$, $\chi_3 = 0.3$, $\chi'_3 = 0.2$, $\chi''_3 = 0.6$, $\chi'_4 = 2.9$, $\chi''_4 = 0.5$, $\chi_5 = 1.9$, $\chi'_5 = 0.5$, $\chi''_5 = 0.7$ and $\tan \beta = 50$. All masses are in GeV and the phases in rad.

In Fig. 8 the dependence of the neutrino magnetic moments on the phase χ_5 is exhibited for three different values of χ'_5 from the upper solid curve down to the short-dashed curve at $\chi_5 = 0$, and $\chi'_5 = 0.5, 1.0, 1.5$ rad. Here one finds that the variation of χ_5 produces a dramatically different effect on μ_1 vs μ_2 . Thus μ_2 has essentially a gentle dependence on χ_5 while μ_1 exhibits a much more rapid variation. Changing χ'_5 does not alter μ_2 by much which is why the curves are nearly overlapping. Over the entire χ_5 range ($0 \rightarrow \pi$ rad), the values of μ_2 stretch from $\sim 2.6 \times 10^{-10} \mu_B$ to $\sim 4.2 \times 10^{-10} \mu_B$ which lie below the current experimental upper bounds but are tantalizingly close to it. The corresponding ν_3 lifetimes are also encouraging. As for μ_1 , its value is very sensitive to variations in the phase χ_5 and a major shift in peaks occurs for the three considered values of χ'_5 . Values in the order of $10^{-13} \mu_B$ are obtained in this parameter space. In the previous analysis shown in figs. 4 and 5, the neutrino masses lie in the required range and thus the three constraints of Eqs. (35)–(37) were satisfied. Here, changing χ_5 will impact the neutrino diagonalizing matrices D_R^ν and D_L^ν and one needs to make certain that the neutrino eigenmasses lie in the acceptable range. In Fig. 8, one finds that for the parameter point $\chi_5 = 1.9$ rad and $\chi'_5 = 0.5$ rad all constraints are satisfied along with desirable values of the ν_3 lifetime, and of μ_2 and μ_1 , i.e., here one has $\mu_2 = 3.6 \times 10^{-10} \mu_B$, $\mu_1 = 1.2 \times 10^{-13} \mu_B$ and $\nu_3 = 8.2 \times 10^{13}$ yrs.



(a) The muon neutrino magnetic moment and tau neutrino lifetime versus χ_5 . (b) The electron neutrino magnetic moment and tau neutrino lifetime versus χ_5 .

Figure 8: A display of the neutrino magnetic moments and the ν_3 lifetime as a function of the phase χ_5 . The left panel gives the ν_2 magnetic moment and the right panel gives the ν_1 magnetic moment along with the ν_3 lifetime. The three curves correspond to $\chi'_5 = 0.5$ (solid), $\chi'_5 = 1.0$ (long dashed), and $\chi'_5 = 1.5$ (short dashed). The marked curves correspond to the ν_3 lifetime. Other parameters have the values $m_2 = 300$, $\mu = 100$, $|f_3| = 7 \times 10^{-8}$, $|f'_3| = 5 \times 10^{-8}$, $|f''_3| = 8 \times 10^{-9}$, $|f_4| = 57$, $|f'_4| = 42$, $|f''_4| = 42$, $|f_5| = 8.11 \times 10^{-2}$, $|f'_5| = 9.8 \times 10^{-2}$, $|f''_5| = 4 \times 10^{-2}$, $m_N = 212$, $m_E = 360$, $m_0 = 300$, $\chi_3 = 0.3$, $\chi'_3 = 0.2$, $\chi''_3 = 0.6$, $\chi_4 = 2.8$, $\chi'_4 = 0.1$, $\chi''_4 = 0.5$, $A_0 = 579$, $\tan \beta = 60$ and $\chi''_5 = 0.7$. All masses are in GeV and the phases in rad.

In summary, the analysis of Figs. 4- 8 shows that the neutrino magnetic moments as low as the current experimental lower limits can be obtained with a vectorlike generation. These magnetic moments are up to 7 orders of magnitude larger than with the Standard Model interactions and within the reach of improved experiment.

Finally we compare our results with some previous works where neutrino magnetic moments much larger than given in Eq.(1) were achieved. Thus the analysis of [41, 42] achieved neutrino magnetic moments as large as $(10^{-17} - 10^{-16})\mu_B$ which are up to five to six orders of magnitude larger than given by Eq.(1) when one uses a generic neutrino mass of 10^{-3} eV in Eq. (1). Our predicted neutrino moments fall in the range $(10^{-12} - 10^{-14})\mu_B$ and are up to $(10^8 - 10^{10})$ orders of magnitude larger than the result of Eq.(1). Further, the analysis of [41, 42] is based on models with explicit R -parity violation and the low energy signatures of such models will have no large missing energy signals which are typically associated with R-parity conserving supersymmetric models. In contrast our analysis is done in extensions of MSSM with R parity conservation. Thus the set up

as well as the predictions of our work are very different from the works of [41, 42].

7 Conclusion

It is well known that the neutrino Dirac magnetic moment computed using the standard model interactions is far too small to be tested by experiment since it would require an increase in sensitivity by several orders of magnitude which appears out of reach in the current and in the near future experiments. Since the neutrino magnetic moment in the standard model is too small to be observed, an observation of a much larger moment will be a clear indication of new physics beyond the standard model. In this work we have carried out an analysis of the neutrino magnetic moments within an extension of MSSM which includes a vectorlike leptonic generation which contains a fourth leptonic generation along with its mirrors. We assume terms in the superpotential of the theory that mix the ordinary leptonic generation with the vectorlike generation. The analysis of the neutrino magnetic moment within this framework shows that a magnetic moment for the neutrinos as large as $(10^{-12} - 10^{-14})\mu_B$ can be obtained. These values thus lie within reach of improved experiment in the future. The analysis is of importance since neutrino magnetic moments have implications for particle physics as well as for astrophysical phenomena, and as already mentioned an observation of it of a size significantly larger than predicted with the standard model like interactions would provide a clear indication of new physics beyond the standard model.

Acknowledgments:

This research was supported in part by the NSF Grant PHY-1314774 and DE-AC02-05CH11231.

8 Appendix: Further details on the scalar mass squared matrices

In this Appendix we give further details of the structure of the slepton mass matrices. The mass terms arising from the superpotential are given by

$$\mathcal{L}_F^{\text{mass}} = \mathcal{L}_C^{\text{mass}} + \mathcal{L}_N^{\text{mass}} , \quad (41)$$

where $\mathcal{L}_C^{\text{mass}}$ gives the mass terms for the charged leptons while $\mathcal{L}_N^{\text{mass}}$ gives the mass terms for the neutrinos. For $\mathcal{L}_C^{\text{mass}}$ we have

$$\begin{aligned}
-\mathcal{L}_C^{\text{mass}} = & \left(\frac{v_2^2 |f_2'|^2}{2} + |f_3|^2 + |f_3'|^2 + |f_3''|^2 \right) \tilde{E}_R \tilde{E}_R^* + \left(\frac{v_2^2 |f_2'|^2}{2} + |f_4|^2 + |f_4'|^2 + |f_4''|^2 \right) \tilde{E}_L \tilde{E}_L^* \\
& + \left(\frac{v_1^2 |f_1|^2}{2} + |f_4|^2 \right) \tilde{\tau}_R \tilde{\tau}_R^* + \left(\frac{v_1^2 |f_1|^2}{2} + |f_3|^2 \right) \tilde{\tau}_L \tilde{\tau}_L^* + \left(\frac{v_1^2 |h_1|^2}{2} + |f_4'|^2 \right) \tilde{\mu}_R \tilde{\mu}_R^* \\
& + \left(\frac{v_1^2 |h_1|^2}{2} + |f_3|^2 \right) \tilde{\mu}_L \tilde{\mu}_L^* + \left(\frac{v_1^2 |h_2|^2}{2} + |f_4''|^2 \right) \tilde{e}_R \tilde{e}_R^* + \left(\frac{v_1^2 |h_2|^2}{2} + |f_3''|^2 \right) \tilde{e}_L \tilde{e}_L^* \\
& + \left\{ -\frac{f_1 \mu^* v_2}{\sqrt{2}} \tilde{\tau}_L \tilde{\tau}_R^* - \frac{h_1 \mu^* v_2}{\sqrt{2}} \tilde{\mu}_L \tilde{\mu}_R^* - \frac{f_2' \mu^* v_1}{\sqrt{2}} \tilde{E}_L \tilde{E}_R^* + \left(\frac{f_2' v_2 f_3^*}{\sqrt{2}} + \frac{f_4 v_1 f_1^*}{\sqrt{2}} \right) \tilde{E}_L \tilde{\tau}_L^* \right. \\
& + \left(\frac{f_4 v_2 f_2'^*}{\sqrt{2}} + \frac{f_1 v_1 f_3^*}{\sqrt{2}} \right) \tilde{E}_R \tilde{\tau}_R^* + \left(\frac{f_3' v_2 f_2'^*}{\sqrt{2}} + \frac{h_1 v_1 f_4'^*}{\sqrt{2}} \right) \tilde{E}_L \tilde{\mu}_L^* + \left(\frac{f_2' v_2 f_4'^*}{\sqrt{2}} + \frac{f_3' v_1 h_1^*}{\sqrt{2}} \right) \tilde{E}_R \tilde{\mu}_R^* \\
& + \left(\frac{f_3'' v_2 f_2'^*}{\sqrt{2}} + \frac{f_4'' v_1 h_2^*}{\sqrt{2}} \right) \tilde{E}_L \tilde{e}_L^* + \left(\frac{f_4' v_2 f_2'^*}{\sqrt{2}} + \frac{f_3'' v_1 h_2^*}{\sqrt{2}} \right) \tilde{E}_R \tilde{e}_R^* + f_3' f_3^* \tilde{\mu}_L \tilde{\tau}_L^* + f_4 f_4^* \tilde{\mu}_R \tilde{\tau}_R^* \\
& \left. + f_4 f_4^* \tilde{e}_R \tilde{\tau}_R^* + f_3'' f_3^* \tilde{e}_L \tilde{\tau}_L^* + f_3' f_3^* \tilde{e}_L \tilde{\mu}_L^* + f_4 f_4^* \tilde{e}_R \tilde{\mu}_R^* - \frac{h_2 \mu^* v_2}{\sqrt{2}} \tilde{e}_L \tilde{e}_R^* + H.c. \right\} \quad (42)
\end{aligned}$$

For $\mathcal{L}_N^{\text{mass}}$ we have

$$\begin{aligned}
-\mathcal{L}_N^{\text{mass}} = & \left(\frac{v_1^2 |f_2|^2}{2} + |f_3|^2 + |f_3'|^2 + |f_3''|^2 \right) \tilde{N}_R \tilde{N}_R^* \\
& + \left(\frac{v_2^2 |f_2|^2}{2} + |f_5|^2 + |f_5'|^2 + |f_5''|^2 \right) \tilde{N}_L \tilde{N}_L^* + \left(\frac{v_2^2 |f_1|^2}{2} + |f_5|^2 \right) \tilde{\nu}_{\tau R} \tilde{\nu}_{\tau R}^* \\
& + \left(\frac{v_2^2 |f_1|^2}{2} + |f_3|^2 \right) \tilde{\nu}_{\tau L} \tilde{\nu}_{\tau L}^* + \left(\frac{v_2^2 |h_1|^2}{2} + |f_3|^2 \right) \tilde{\nu}_{\mu L} \tilde{\nu}_{\mu L}^* + \left(\frac{v_2^2 |h_1|^2}{2} + |f_5|^2 \right) \tilde{\nu}_{\mu R} \tilde{\nu}_{\mu R}^* \\
& + \left(\frac{v_2^2 |h_2|^2}{2} + |f_3|^2 \right) \tilde{\nu}_{eL} \tilde{\nu}_{eL}^* + \left(\frac{v_2^2 |h_2|^2}{2} + |f_5''|^2 \right) \tilde{\nu}_{eR} \tilde{\nu}_{eR}^* \\
& + \left\{ -\frac{f_2 \mu^* v_2}{\sqrt{2}} \tilde{N}_L \tilde{N}_R^* - \frac{f_1 \mu^* v_1}{\sqrt{2}} \tilde{\nu}_{\tau L} \tilde{\nu}_{\tau R}^* - \frac{h_1' \mu^* v_1}{\sqrt{2}} \tilde{\nu}_{\mu L} \tilde{\nu}_{\mu R}^* + \left(\frac{f_5 v_2 f_1'^*}{\sqrt{2}} - \frac{f_2 v_1 f_3^*}{\sqrt{2}} \right) \tilde{N}_L \tilde{\nu}_{\tau L}^* \right. \\
& + \left(\frac{f_5 v_1 f_2^*}{\sqrt{2}} - \frac{f_1' v_2 f_3^*}{\sqrt{2}} \right) \tilde{N}_R \tilde{\nu}_{\tau R}^* + \left(\frac{h_1' v_2 f_5'^*}{\sqrt{2}} - \frac{f_3' v_1 f_2^*}{\sqrt{2}} \right) \tilde{N}_L \tilde{\nu}_{\mu L}^* + \left(\frac{f_5'' v_1 f_2^*}{\sqrt{2}} - \frac{f_3'' v_2 h_2^*}{\sqrt{2}} \right) \tilde{N}_R \tilde{\nu}_{eR}^* \\
& + \left(\frac{h_2^* v_2 f_5''}{\sqrt{2}} - \frac{f_3'' v_1 f_2^*}{\sqrt{2}} \right) \tilde{N}_L \tilde{\nu}_{eL}^* + \left(\frac{f_5' v_1 f_2^*}{\sqrt{2}} - \frac{h_1' v_2 f_3'^*}{\sqrt{2}} \right) \tilde{N}_R \tilde{\nu}_{\mu R}^* \\
& + f_3' f_3^* \tilde{\nu}_{\mu L} \tilde{\nu}_{\tau L}^* + f_5 f_5^* \tilde{\nu}_{\mu R} \tilde{\nu}_{\tau R}^* - \frac{h_2' \mu^* v_1}{\sqrt{2}} \tilde{\nu}_{eL} \tilde{\nu}_{eR}^* \\
& \left. + f_3'' f_3^* \tilde{\nu}_{eL} \tilde{\nu}_{\tau L}^* + f_5 f_5^* \tilde{\nu}_{eR} \tilde{\nu}_{\tau R}^* + f_3' f_3^* \tilde{\nu}_{eL} \tilde{\nu}_{\mu L}^* + f_5 f_5^* \tilde{\nu}_{eR} \tilde{\nu}_{\mu R}^* + H.c. \right\}.
\end{aligned}$$

We define the scalar mass squared matrix $M_{\tilde{\tau}}^2$ in the basis $(\tilde{\tau}_L, \tilde{E}_L, \tilde{\tau}_R, \tilde{E}_R, \tilde{\mu}_L, \tilde{\mu}_R, \tilde{e}_L, \tilde{e}_R)$. We label the matrix elements of these as $(M_{\tilde{\tau}}^2)_{ij} = M_{ij}^2$ where the elements of the matrix are given by

$$\begin{aligned}
M_{11}^2 &= \tilde{M}_{\tau L}^2 + \frac{v_1^2 |f_1|^2}{2} + |f_3|^2 - m_Z^2 \cos 2\beta \left(\frac{1}{2} - \sin^2 \theta_W \right), \\
M_{22}^2 &= \tilde{M}_E^2 + \frac{v_2^2 |f_2'|^2}{2} + |f_4|^2 + |f_4'|^2 + |f_4''|^2 + m_Z^2 \cos 2\beta \sin^2 \theta_W, \\
M_{33}^2 &= \tilde{M}_{\tau}^2 + \frac{v_1^2 |f_1|^2}{2} + |f_4|^2 - m_Z^2 \cos 2\beta \sin^2 \theta_W, \\
M_{44}^2 &= \tilde{M}_{\chi}^2 + \frac{v_2^2 |f_2'|^2}{2} + |f_3|^2 + |f_3'|^2 + |f_3''|^2 + m_Z^2 \cos 2\beta \left(\frac{1}{2} - \sin^2 \theta_W \right), \\
M_{55}^2 &= \tilde{M}_{\mu L}^2 + \frac{v_1^2 |h_1|^2}{2} + |f_3'|^2 - m_Z^2 \cos 2\beta \left(\frac{1}{2} - \sin^2 \theta_W \right), \\
M_{66}^2 &= \tilde{M}_{\mu}^2 + \frac{v_1^2 |h_1|^2}{2} + |f_4'|^2 - m_Z^2 \cos 2\beta \sin^2 \theta_W, \\
M_{77}^2 &= \tilde{M}_{eL}^2 + \frac{v_1^2 |h_2|^2}{2} + |f_3''|^2 - m_Z^2 \cos 2\beta \left(\frac{1}{2} - \sin^2 \theta_W \right), \\
M_{88}^2 &= \tilde{M}_e^2 + \frac{v_1^2 |h_2|^2}{2} + |f_4''|^2 - m_Z^2 \cos 2\beta \sin^2 \theta_W, \\
M_{12}^2 &= M_{21}^{2*} = \frac{v_2 f_2' f_3^*}{\sqrt{2}} + \frac{v_1 f_4 f_1^*}{\sqrt{2}}, \\
M_{13}^2 &= M_{31}^{2*} = \frac{f_1^*}{\sqrt{2}} (v_1 A_{\tau}^* - \mu v_2), \\
M_{14}^2 &= M_{41}^{2*} = 0, M_{15}^2 = M_{51}^{2*} = f_3' f_3^*, \\
M_{16}^{2*} &= M_{61}^{2*} = 0, M_{17}^{2*} = M_{71}^{2*} = f_3'' f_3^*, M_{18}^{2*} = M_{81}^{2*} = 0, M_{23}^2 = M_{32}^{2*} = 0, \\
M_{24}^2 &= M_{42}^{2*} = \frac{f_2'^*}{\sqrt{2}} (v_2 A_E^* - \mu v_1), M_{25}^2 = M_{52}^{2*} = \frac{v_2 f_3' f_2'^*}{\sqrt{2}} + \frac{v_1 h_1 f_4^*}{\sqrt{2}}, \\
M_{26}^2 &= M_{62}^{2*} = 0, M_{27}^2 = M_{72}^{2*} = \frac{v_2 f_3'' f_2'^*}{\sqrt{2}} + \frac{v_1 h_1 f_4'^*}{\sqrt{2}}, M_{28}^2 = M_{82}^{2*} = 0, \\
M_{34}^2 &= M_{43}^{2*} = \frac{v_2 f_4 f_2'^*}{\sqrt{2}} + \frac{v_1 f_1 f_3^*}{\sqrt{2}}, M_{35}^2 = M_{53}^{2*} = 0, M_{36}^2 = M_{63}^{2*} = f_4 f_4'^*, \\
M_{37}^2 &= M_{73}^{2*} = 0, M_{38}^2 = M_{83}^{2*} = f_4 f_4'^*, M_{45}^2 = M_{54}^{2*} = 0, M_{46}^2 = M_{64}^{2*} = \frac{v_2 f_2' f_4'^*}{\sqrt{2}} + \frac{v_1 f_3' h_1^*}{\sqrt{2}}, \\
M_{47}^2 &= M_{74}^{2*} = 0, M_{48}^2 = M_{84}^{2*} = \frac{v_2 f_2' f_4''^*}{\sqrt{2}} + \frac{v_1 f_3'' h_2^*}{\sqrt{2}}, \\
M_{56}^2 &= M_{65}^{2*} = \frac{h_1^*}{\sqrt{2}} (v_1 A_{\mu}^* - \mu v_2), M_{57}^2 = M_{75}^{2*} = f_3'' f_3'^*, M_{58}^2 = M_{85}^{2*} = 0, M_{67}^2 = M_{76}^{2*} = 0, \\
M_{68}^2 &= M_{86}^{2*} = f_4' f_4'^*, M_{78}^2 = M_{87}^{2*} = \frac{h_2^*}{\sqrt{2}} (v_1 A_e^* - \mu v_2)
\end{aligned} \tag{43}$$

Here the terms $M_{11}^2, M_{13}^2, M_{31}^2, M_{33}^2$ arise from soft breaking in the sector $\tilde{\tau}_L, \tilde{\tau}_R$, the terms $M_{55}^2, M_{56}^2, M_{65}^2, M_{66}^2$ arise from soft breaking in the sector $\tilde{\mu}_L, \tilde{\mu}_R$, the terms $M_{77}^2, M_{78}^2, M_{87}^2, M_{88}^2$ arise from soft breaking in the sector \tilde{e}_L, \tilde{e}_R and the terms $M_{22}^2, M_{24}^2, M_{42}^2, M_{44}^2$ arise from soft breaking in the sector \tilde{E}_L, \tilde{E}_R . The other terms arise from mixing between the staus, smuons and the mirrors. We assume that all the masses are of the electroweak size so all the terms enter in the mass squared matrix. We diagonalize this hermitian mass squared matrix by the unitary transformation $\tilde{D}^{\tau\dagger} M_{\tilde{\tau}}^2 \tilde{D}^{\tau} = \text{diag}(M_{\tilde{\tau}_1}^2, M_{\tilde{\tau}_2}^2, M_{\tilde{\tau}_3}^2, M_{\tilde{\tau}_4}^2, M_{\tilde{\tau}_5}^2, M_{\tilde{\tau}_6}^2, M_{\tilde{\tau}_7}^2, M_{\tilde{\tau}_8}^2)$. For a further clarification of the notation see [23].

References

- [1] K. Fujikawa and R. Shrock, Phys. Rev. Lett. **45** (1980) 963.
- [2] W. J. Marciano and A. I. Sanda, Phys. Lett. B **67** (1977) 303; B. W. Lee and R. E. Shrock, Phys. Rev. D **16** (1977) 1444.
- [3] C. Arpesella *et al.* [The Borexino Collaboration], Borexino Data,” Phys. Rev. Lett. **101** (2008) 091302. [arXiv:0805.3843 [astro-ph]].
- [4] D. Montanino, M. Picariello and J. Pulido, Phys. Rev. D **77** 093011(2008) [arXiv:0801.2643 [hep-ph]].
- [5] H. T. Wong *et al.* [TEXONO Collaboration], Phys. Rev. D **75**, 012001 (2007) [hep-ex/0605006].
- [6] A. G. Beda, V. B. Brudanin, V. G. Egorov, D. V. Medvedev, V. S. Pogosov, M. V. Shirchenko and A. S. Starostin, Adv. High Energy Phys. **2012**, 350150 (2012).
- [7] A. G. Beda, E. V. Demidova, A. S. Starostin, V. B. Brudanin, V. G. Egorov, D. V. Medvedev, M. V. Shirchenko and T. Vylov, Phys. Part. Nucl. Lett. **7**, 406 (2010) [arXiv:0906.1926 [hep-ex]]; A. G. Beda, V. B. Brudanin, V. G. Egorov, D. V. Medvedev, V. S. Pogosov, M. V. Shirchenko and A. S. Starostin, arXiv:1005.2736 [hep-ex].
- [8] G. G. Raffelt, Phys. Rev. Lett. **64** (1990) 2856.
- [9] J. Beringer *et al.* [Particle Data Group Collaboration], Phys. Rev. D **86**, 010001 (2012).

- [10] N. F. Bell, V. Cirigliano, M. J. Ramsey-Musolf, P. Vogel and M. B. Wise, Phys. Rev. Lett. **95**, 151802 (2005) [hep-ph/0504134].
- [11] A. B. Balantekin, AIP Conf. Proc. **847**, 128 (2006) [hep-ph/0601113].
- [12] K. A. Kouzakov, A. I. Studenikin and M. B. Voloshin, J. Phys. Conf. Ser. **375**, 042045 (2012) [arXiv:1112.4050 [hep-ph]].
- [13] C. -Q. Geng and R. Takahashi, Phys. Lett. B **710**, 324 (2012) [arXiv:1201.1534 [hep-ph]].
- [14] H. T. Wong and H. -B. Li, Mod. Phys. Lett. A **20**, 1103 (2005).
- [15] C. Brogini, C. Giunti and A. Studenikin, Adv. High Energy Phys. **2012**, 459526 (2012) [arXiv:1207.3980 [hep-ph]].
- [16] C. Giunti and A. Studenikin, Phys. Atom. Nucl. **72**, 2089 (2009) [arXiv:0812.3646 [hep-ph]]; A. Studenikin, Nucl. Phys. Proc. Suppl. **188** (2009) 220.
- [17] H. Georgi, Nucl. Phys. B **156**, 126 (1979); F. Wilczek and A. Zee, Phys. Rev. D **25**, 553 (1982); J. Maalampi, J.T. Peltoniemi, and M. Roos, PLB 220, 441(1989); J. Maalampi and M. Roos, Phys. Rept. **186**, 53 (1990); K. S. Babu, I. Gogoladze, P. Nath and R. M. Syed, Phys. Rev. D **72**, 095011 (2005) [hep-ph/0506312]; Phys. Rev. D **74**, 075004 (2006), [arXiv:hep-ph/0607244]; Phys. Rev. D **85**, 075002 (2012) [arXiv:1112.5387 [hep-ph]]; P. Nath and R. M. Syed, Phys. Rev. D **81**, 037701 (2010).
- [18] A. Aboubrahim, T. Ibrahim and P. Nath, Phys. Rev. D **88**, 013019 (2013) [arXiv:1306.2275 [hep-ph]].
- [19] T. Ibrahim and P. Nath, Phys. Rev. D **78**, 075013 (2008) [arXiv:0806.3880 [hep-ph]].
- [20] T. Ibrahim and P. Nath, Phys. Rev. D **81**, 033007 (2010) [arXiv:1001.0231 [hep-ph]].
- [21] T. Ibrahim and P. Nath, Phys. Rev. D **84**, 015003 (2011) [arXiv:1104.3851 [hep-ph]].
- [22] T. Ibrahim and P. Nath, Phys. Rev. D **82**, 055001 (2010) [arXiv:1007.0432 [hep-ph]].
- [23] T. Ibrahim and P. Nath, Phys. Rev. D **87**, 015030 (2013) [arXiv:1211.0622 [hep-ph]].
- [24] T. Ibrahim and P. Nath, Nucl. Phys. Proc. Suppl. **200-202**, 161 (2010) [arXiv:0910.1303 [hep-ph]].

- [25] K. S. Babu, I. Gogoladze, M. U. Rehman and Q. Shafi, Phys. Rev. D **78**, 055017 (2008).
- [26] C. Liu, Phys. Rev. D **80**, 035004 (2009) [arXiv:0907.3011 [hep-ph]].
- [27] S. P. Martin, Phys. Rev. D **81**, 035004 (2010) [arXiv:0910.2732 [hep-ph]].
- [28] J. L. Hewett, H. Weerts, R. Brock, J. N. Butler, B. C. K. Casey, J. Collar, A. de Gouvea and R. Essig *et al.*, arXiv:1205.2671 [hep-ex].
- [29] G. C. McLaughlin and J. N. Ng, Phys. Lett. B **470**, 157 (1999) [hep-ph/9909558].
- [30] R. N. Mohapatra, S. -P. Ng and H. -b. Yu, Phys. Rev. D **70**, 057301 (2004) [hep-ph/0404274].
- [31] P. A. R. Ade *et al.* [Planck Collaboration], arXiv:1303.5062 [astro-ph.CO].
- [32] T. Schwetz, M. A. Tortola and J. W. F. Valle, New J. Phys. **10**, 113011 (2008) [arXiv:0808.2016 [hep-ph]]. See also M. C. Gonzalez-Garcia, M. Maltoni, J. Salvado and T. Schwetz, JHEP **1212**, 123 (2012) [arXiv:1209.3023 [hep-ph]].
- [33] P. B. Pal and L. Wolfenstein, Phys. Rev. D **25**, 766 (1982); K. Sato and M. Kobayashi, Prog. Theor. Phys. **58**, 1775 (1977); R. E. Shrock, Nucl. Phys. B **206**, 359 (1982); M. A. B. Beg, W. J. Marciano and M. Ruderman, Phys. Rev. D **17**, 1395 (1978).
- [34] S. Matsuura, M. Shirahata, M. Kawada, T. T. Takeuchi, D. Burgarella, D. L. Clements, W. -S. Jeong and H. Hanami *et al.*, Astrophys. J. **737**, 2 (2011) [arXiv:1002.3674 [astro-ph.CO]].
- [35] H. Dole, G. Lagache, J. -L. Puget, K. I. Caputi, N. Fernandez-Conde, E. Le Floc'h, C. Papovich and P. G. Perez-Gonzalez *et al.*, Astron. Astrophys. **451**, 417 (2006) [astro-ph/0603208].
- [36] S. Berta, B. Magnelli, D. Lutz, B. Altieri, H. Aussel, P. Andreani, O. Bauer and A. Bongiovanni *et al.*, arXiv:1005.1073 [astro-ph.CO].
- [37] A. Mirizzi, D. Montanino and P. D. Serpico, Phys. Rev. D **76**, 053007 (2007) [arXiv:0705.4667 [hep-ph]].
- [38] S. -H. Kim, K. -i. Takemasa, Y. Takeuchi and S. Matsuura, J. Phys. Soc. Jap. **81**, 024101 (2012) [arXiv:1112.4568 [hep-ph]].
- [39] T. Ibrahim and P. Nath, Rev. Mod. Phys. **80**, 577 (2008) [arXiv:0705.2008 [hep-ph]]; A. Pilaftsis, hep-ph/9908373.

- [40] T. Ibrahim and P. Nath, Phys. Rev. D **62**, 015004 (2000) [hep-ph/9908443]; Phys. Rev. D **61**, 095008 (2000) [hep-ph/9907555];
- [41] M. Gozdz, W. A. Kaminski, F. Simkovic and A. Faessler, Phys. Rev. D **74**, 055007 (2006) [hep-ph/0606077].
- [42] M. Gozdz, W. A. Kaminski and F. Simkovic, Int. J. Mod. Phys. E **15**, 441 (2006) [arXiv:1201.1237 [hep-ph]].